Effective microbial calcite precipitation by a new mutant and precipitating regulation of extracellular urease

Hui Li, Youxin Song, Qijiu Li, Jianwei He, Youtao Song

PII: S0960-8524(14)00855-4
DOI: http://dx.doi.org/10.1016/j.biortech.2014.06.011
Reference: BITE 13545

To appear in: *Bioresource Technology*

Received Date: 9 March 2014
Revised Date: 2 June 2014
Accepted Date: 4 June 2014

Please cite this article as: Li, H., Song, Y., Li, Q., He, J., Song, Y., Effective microbial calcite precipitation by a new mutant and precipitating regulation of extracellular urease, *Bioresource Technology* (2014), doi: http://dx.doi.org/10.1016/j.biortech.2014.06.011

Effective microbial calcite precipitation by a new mutant and precipitating regulation of extracellular urease

Hui Li[a], Youxin Song[c], Qijiu Li[a], Jianwei He[a], Youtao Song[a,b,*]

[a] Province Key Laboratory of Animal Resource and Epidemic Disease Prevention, School of Life Science, Liaoning University, Shenyang, 110036, China

[b] School of Environmental Science, Liaoning University, Shenyang, 110036, China

[c] Affiliated Hospital, Chengde Medical University, Chengde, 067000, China

Abstract

Microbial calcite precipitation is a promising and environmental friendly biological technology in remediation of the surface and subsurface of porous media, especially for in-situ soil remediation. The present study isolate a urea-degrading strain LH1 from soil on soybean root, identified as *Bacillus niabensis* strain (99% similarity) by 16S rRNA gene sequencing analysis. Then, using ultraviolet mutagenesis method, a mutant LHUM107 with outstanding urease-producing ability was further obtained to study its effects on calcite precipitation. The mutant LHUM107 had good genome stability and exhibited 92.2% urea-degrading efficiency till 21st generation. Response surface methodology (RSM) noted that the urea degradation was more dependent on initial urea addition, and brought forward the optimal conditions. Adapting to these optimal conditions, calcite precipitation by mutant LHUM107 and extracellular urease was respectively further investigated. It was shown that extracellular urease excreted from mutant LHUM107 was more effective and more targeted for $CaCO_3$ precipitation.

Key words: microbial calcite precipitation; urea-degrading; extracellular urease; *Bacillus*; 16S rRNA gene sequencing

*Correspondence author: Province Key Laboratory of Animal Resource and Epidemic Disease Prevention, School of Life Science, Liaoning University, Shenyang, 110036, China. Tel: +86-024-62202682; E-mail address: ysong@lnu.edu.cn.

1. Introduction

Microbial precipitation of carbonate, mainly $CaCO_3$, is a bioreaction occurred widely in nature. Marine animals and plants (Rahman *et al.*, 2008), algae (De Beer and Larkum, 2011) and microorganisms were all found to have the capability to mediate the precipitation of $CaCO_3$. In particular, $CaCO_3$ precipitation induced by microorganisms played a very important role in the entire biological mineralization sediments (Riding, 2000). The cementation function of microbiologically generated $CaCO_3$ had a potential in the remediation of the surface and subsurface of porous media (Stocks-Fischer *et al.*, 1999), e.g., the cementation of sandy materials, crack and fissure remediation of stones, protective remediation of stone-sculpted relics and also soil amelioration (Jiménez-López *et al.*, 2007; Soon *et al.*, 2013). Based on these, the technology has been considered as a creative environment-friendly biotechnology (Kim *et al.*, 2013), and therefore a focus of research interest in the area of environmental engineering.

At present, the microbial precipitation of $CaCO_3$ is believed to occur via two pathways: (1) urea degrading bacteria excrete urease to catalyze the degradation of urea and produce CO_2 and NH_3. As the hydrolysis of NH_3 produces NH_4^+-N leading to an increase in the pH of the solution, CO_2 and calcium ions get precipitated to form $CaCO_3$ (Stocks-Fischer *et al.*, 1999). For example, $CaCO_3$ precipitation can be induced in artificial groundwater systems by *Bacillus pasteurii* mediated urea hydrolysis (Ferris *et al.*, 2004). (2) Some microorganisms induce extracellular precipitation of carbonate by a series of comprehensive bioprocesses (Baskar *et al.*, 2006), e.g., photosynthesis, ammoxification, denitrification, sulfate reduction and anaerobic sulfide oxidation, etc.

It should be noted that the non-hydrated $CaCO_3$ crystals include calcite, aragonite and

vaterite, which differ largely in the structure stability (Rivadeneyra *et al.*, 2000). Previous research demonstrated that *Myxococcus xanthus*, a commonly seen soil bacterium, tends to promote the formation of the unstable vaterite crystals (Rodriguez-Navarro *et al.*, 2007). Therefore, process control needs to be introduced to navigate the production of calcite or aragonite, especially calcite as the most stable crystal for the purpose of biological mineralization. *Bacillus pasteurii* is capable of inducing the precipitation of calcite crystals (DeJong *et al.*, 2006) and thus becomes the most widely used strain. Except *Bacillus pasteurii*, there were not many functional strains for mediating calcite crystal precipitation being reported. The limited microbe resource is now one of the main problems confronted in the area. Based on the recent literature, all the application of *Bacillus pasteurii* was via direct dosing the bacteria suspension (Cheng and Cord-Ruwisch, 2012). However, the living bacteria consist mainly of water and organic compounds, which will be too fragile to be the inner core for stable precipitation of $CaCO_3$. In addition, as for aerobic urease-producing strains, aeration will be needed to support their metabolic activity in real application. Limited oxygen supply would reduce the urease production.

This study screened strains capable of producing extracellular urease from the soil near soybean root. To advance urea-degrading capability, a mutant was induced by ultraviolet mutagenesis. Furthermore, after optimizing of urea degrading capability of the mutant by response surface methodology (RSM), extracellular urease was collected for $CaCO_3$ precipitation. The study provides a new sight to the application of biological mineralization and also new bacterium sources with extracellular urease producing capacity.

2. Materials and Methods

2.1 Starting strain and its mutagenesis

The starting strain was obtained from the soil near soybean roots. After passing through a 60-mesh screen, 1 g of soil samples were added in 500 ml Erlenmeyer flasks loading with 200 ml of selective broth and 20 2-mm glass beans. The flasks were then placed in a 30 °C thermostat shaker at an agitation rate of 150 rpm for 72 h. The screening broth was modified from recipe proposed in Stocks-Fischer *et al.* (1999), taking urea as the sole nitrogen source. The components included (per liter): peptone 5g, urea 10 g, NaCl 10 g, KH_2PO_4 0.5 g, pH 6.8. The selective medium was autoclaved at 121 °C for 30 min. The soil suspension (1 ml) was sampled via gradient dilution using 0.9% NaCl solution, and the diluent (100 μl) was streaked on selective medium plate, which was then incubated at 30 °C. According to the surrounding color of colonies, the available strains with urea-degrading ability were screened. Then, such above procedures were repeated until a strain high capable of degrading urea was obtained, named as LH1. The solid medium was prepared by adding 0.001 g l^{-1} of phenolphthalein and 20 g l^{-1} of agar into the selective broth, in which phenolphthalein was the abdicator of pH increase caused by the urea decompose-resulted NH_3 production.

The mutagenesis was conducted according to the protocol described in Witkin (1976). The bacterial suspension (3 ml) of LH1 with concentration of 1.8×10^8 cells ml^{-1} was added to sterile petri dish (9 cm) with rotator in the middle, then being placed on a magnetic stirrer at a low speed. A 30 W UV light was placed at 30 cm from the petri dish. The cell suspension of 100 μl was sampled under the protection of infrared light at 1 min-interval for 15 times. The suspension was spread on the medium plates, which were then wrapped with black sheet before being incubated at 30 °C. Repeated mutagenesis and cultivation were done until a mutant strain with high capability of extracellular urease expression was obtained out of the 282 strains by testing their reproduction

rate, urea degradation capability and the genome stability. The obtained strain was finally named as LHUM107.

2.2 16S rRNA gene sequences and phylogenetic analysis of starting strain LH1

2.2.1 DNA extraction and PCR amplification

DNA extraction was performed according to previous protocol mentioned in Wan *et al.* (2011). The bacterial suspension (3 ml) was centrifuged at 10,000 g for 3 min to concentrate bacterium. The supernatant was discarded. The genomic DNA (100 μl) of starting strain was extracted from precipitates using PowerSoil DNA isolation kit (Mobic Inc, USA).

The V3 region of 16S rRNA was amplified by polymerase chain reaction (PCR) using universal bacterial primers (8F, 5´-AGAGTTTGATCCTGGCTCAG-3´ and 1541R, 5´-GCTGCCTCCCGTAGGAGT-3´). The collected DNA was mixed with a polymerase chain reaction (PCR) mixture (100 μl): 10 μl 10× LA Taq buffer, 16 μl of dNTP mixture (2.5 mM), 3 μl 8F-primer (20 μM), 3 μl 1541R-primer (20 μM), 4 μl DNA template, 10 U LA Taq DNA polymerase, and sterile ddH_2O to a final volume of 100 μl. The PCR conditions were as follow: 95 °C for 10 min, followed by 30 denaturation cycles at 95 °C for 1 min, annealing at 55 °C for 1 min, and elongation at 72 °C for 1.5 min, followed by final extension at 72 °C for 10 min. The genomic DNA and PCR products were analyzed by electrophoresis in 1% agarose gels.

2.2.2 Cloning and sequencing

The PCR products (80 μl) were purified using the 1% Agarose Gel DNA Purification Kit, ligated into vector pMD18, and transformed into *Escherichia.coli* DH5α. with ampicillin selection and blue/white screening. Positive clones were randomly selected and sequenced by a DNA sequencer (ABI3730, Applied Biosystems, USA). The closet matching sequences in the GenBank

database were searched using the BLAST program. Then the phylogenetic tree was constructed with MEGA4.1 using the neighbor joining algorithm. All the chemicals were purchased from Takara Co., Ltd (Dalian, China).

2.3 Growth and metabolism of mutant strain and its stability

The mutant strain LHUM107 of 10 ml was sampled during the log phase, then centrifuged at 10000 g for 3 min. The precipitate was kept and resuspended with 5 ml of 1× phosphate buffered saline (PBS) solution, then centrifuged at 10000 g for 3 min. The pellets were diluted for three times using 1×PBS solution, and were finally added to 1 ml NaCl (0.9%). The resulted solution was inoculated into 1 l Erlenmeyer flask containing 300 ml of selective broth (same as addressed in 2.1) and was cultivated in a 30 °C thermostat shaker at 150 rpm. The optical density (600 nm) of the bacteria and the urea-degradation efficiency were measured at particular time intervals.

2.4 Optimization of urease expression based on response surface methodology (RSM)

The response surface methodology was used to evaluate the effect of three important factors affecting urea degradation efficiency. The temperature (X_1), urea (X_2), and peptone (X_3) as operating parameters were selected to study their effects on degradation. The effect of each variable on urea degradation was studied at three different coded levels (-1, 0 and +1) with low, medium and high value (Table 1) using the central composite design analysis. This was followed by the analysis using the second-order polynomial equation as Eq.(1):

$$Y = \beta_0 + \sum \beta_n X_n + \sum \beta_{nn} X_n^2 + \sum \beta_{nm} X_n X_m \quad (1)$$

Where, Y is the predicted response, β_0 offset term, β_n liner coefficient, β_{nn} squared coefficient, β_{nm} interaction coefficient, X_n nth independent variable, X_n^2 squared effect and X_nX_m interaction effects. For the three variable systems, the equation is as Eq.(2):

$$Y = \beta_0 + \beta_1 X_1 + \beta_2 X_2 + \beta_3 X_3 + \beta_{11} X_1^2 + \beta_{22} X_2^2 + \beta_{33} X_3^2 + \beta_{12} X_1 X_2 + \beta_{13} X_1 X_3 + \beta_{23} X_2 X_3 \quad (2)$$

After checking the validity of the model, the equation was then used to plot the three dimensional response surfaces, contour plot and analyzed experimental data.

2.5 Calcite precipitates

2.5.1 Calcite precipitates by mutant strains

According to the optimized conditions of urease expression addressed in 2.4, the concentrations of urea, peptone and $CaCl_2$ in broth were altered to be 5.6 g l^{-1}, 8.1 g l^{-1}, and 11.1 g l^{-1}, respectively. After reaching the middle-log phase, 3% of mutant LHUM107 was inoculated into 200 ml broth and then was cultivated under the some conditions described in 2.1. After 48 h, the cell suspension was centrifuged at 10,000 g for 3 min, and resulted pellets were used for following analysis.

2.5.2 Calcite precipitates using extracellular urease from mutant LHUM107

The urea and peptone in broth were added at dosage of 5.6 g l^{-1} and 8.1 g l^{-1}, respectively. The mutant LHUM107, at its mid-log phase, was inoculated into 200 ml of broth under the optimal conditions addressed in 2.4. After 48 h of cultivation, the suspension was centrifuged at 10,000 g for 3 min. The supernatant was collected for extracellular enzyme extraction as described in Rokita *et al.* (2000). The purified enzyme was resuspended in 200 ml ddH_2O with 1.12 g of urea and 2.22 g of $CaCl_2$, and was placed in a 30 °C thermostat shaker at 150 rpm for 12 h. The concentration of Ca^{2+} was followed at particular time intervals. The precipitates were analyzed using scanning electronic microscopy (SEM) and X-ray diffraction (XRD) after 10,000 g centrifuge.

2.6 Other analytical methods

The micro-appearances were observed by scanning electron microscopy (SEM), and the dehydration method for SEM was referred to Wu *et al.* (2010). The analysis of precipitates was conducted using a XRD diffratometer (Bruker-D8 Advance, USA). The concentration of urea in broth was determined according to the method reported in Thomas and Chamberlin (1974). The extracellular Ca^{2+} concentration was monitored using HITACHI P-4010 inductively coupled plasma (ICP).

3. Results and Discussion

3.1 Identification and phylogenetic analysis of starting strain

The morphology of the starting strain LH1 was observed by SEM, and it was exhibited as a short rod-shaped of Gram-positive bacterium, and its size was approximately 0.5×1.3 μm. Fig.1 shows the Neighbor-joining phylogenic tree prepared using LH1 gene fragment and GenBank database sequences. The starting strain was most similar (99% similarity) to *Bacillus niabensis* of *Firmicutes* phylum. The bootstrap values of phylogenic tree was 1000 at the branch points, and 100% of the confidence interval was consequently received, suggesting that evolutionary estimation of LH1 was 100% reliable. In phylogenic tree, *B.pasteurii* had 96% of similarity with LH1, which was noted as a effective urea degrading bacterium (DeJong *et al.*, 2006). This suggests that these two strains were belonging to the same genus. Consequently, LH1 was another strain of *Bacillus* genus found to have urease expression capacity and was able to excrete urease out of cells, providing an alternative species for the application of bio-mineralization technology.

3.2 Growth and metabolism of the mutant LHUM107 and the genome stability

A mutant LHUM107, with a higher urease producing capacity, was obtained after the mutation of starting strain LH1 performed by UV light. With an initial concentration of urea of

10000 mg l^{-1}, the urea-degradation efficiency by LH1 was 67.3% after 5 d of cultivation, while in terms of LHUM107 the value was > 97%. The growth and metabolizing properties of LHUM107 was shown in Fig. 2A. During the in initial period (0-4 h), the bacteria were in the adaptation phase; the concentration of the cells was low and the degradation of urea was insignificant. In the 8th hour, the strain started the log phase, reproducing rapidly. The urea in the medium decreased slightly from 10049.30 mg l^{-1} to 9573.21 mg l^{-1}. During the assays, urea was added as the sole nitrogen source, and it has to be degraded to NH_4^+-N before being used by the microorganisms (Mobley and Hausinger, 1989). For the lag phase, the mutants adapt themselves to growth conditions, particularly in synthesis of urease. When it came to the later log phase, the urease was started to accumulate, and then the growth rate of population increase doubles with this time period.

As a result, urea was rapidly degraded. At the 48th hour, the concentration of urea was reduced from the initial 9573.21 mg l^{-1} to 2108.71 mg l^{-1}, with a removal efficiency of 78%. At this time, the bacteria entered the stationary phase, while the degradation of urea continued. The concentration of urea in the medium was only 139.11 mg l^{-1} at the 120th hour. The growth curve of mutant LHUM107 in the entire assay exhibited an S shape. Based on the logistic model for microbial growth (Verhulst, 1838), the growth curve can be described by Eq. (3).

$$y_{OD} = \frac{2.45}{1+32.26\times e^{-0.18t}} \qquad (3)$$

where, t denotes the growth time, y_{OD} denotes the OD value of the bacteria. According to Logistic model fitting of the growth process (Thornley and France, 2005), the maximum growth rate of the strain in this study was calculated to be 0.18 h^{-1}. In other words, the generation time for mutant LHUM107 was roughly 5.6 h. Urea as the sole indirect

nitrogen source induced the synthesis of urease, which is an urgent regulating of microorganisms under nutriuents' pressure. Thus, a delay of urease synthesis was observed during the adaptation and initial log phase, leading to the degradation of urea being later than the strain growth.

Based on the growth curve, the stationary phase of LHUM107 growth started at the 48th hour. Thus, a continuous cultivation was carried out with a generation time of 48 h. The genome stability related to the urease synthesis capacity of the mutant LHUM107 in the log phase was investigated using urea degrading capacity as an indicator. As shown in Fig. 2B, during the 21 generation, the highest removal efficiency was 96.7%, the lowest of 86.4% and an average of 92.2%. This demonstrated the mutant LHUM107 had considerable genome stability in urease synthesis.

3.3 Optimization of urease synthesis by mutant LHUM107

Response surface methodology (RSM) is a useful model for studying the effect of several factors influencing the process for seeking the optimal conditions. The approach reduces the amount of experiments, improves statistical interpretation possibilities, and indicates the interaction between multiple variables (Jaliliannosrati *et al.*, 2013; Zhou *et al.*, 2013). Urease is an induced enzyme. Urea, as an inducing agent, imposes an important effect on the urease capacity of the strain (Nakano *et al.*, 1984). Analysis of variance (ANOVA) for response surface quadratic model for the urea degradation efficiency was used to justify the adequacy of the models (Montgomery, 2005). The ANOVA for conversion quadric model is summarized in Table 2. The least square regression was used to fit the obtained results. As can be seen in Table 2, the F-value of 5.12 implied that the quadratic model was significant. Moreover, each term in the model was

also tested for significance. A p-value smaller than 0.05 implies that correspond model term is significant, and there is only a 0.88% chance than a "Model F-Value" this large could occur due to noise. From Table 2, it is evident that the linear terms for temperature (X_1) and urea (X_2) have large effects on the urea degradation efficiency due to high F-values. The quadratic term for the urea (X_2) has a large F-value. Thus, the effect of urea on the urea degradation efficiency strongly modeled with the quadratic term.

Based on urea degradation efficiency, a complete quadratic model was utilized to fit the experimental data. Since the units of three variables are different in this study, coefficients for coded factors are utilized as shown in Eq. (4) to represent urea degradation efficiency as a response surface.

$$Y\text{ (urea degradation efficiency)} = 94.36 - 2.61X_1 + 8.48X_2 + 11.37X_3 + 4.58X_1X_2 + 4.65X_1X_3 - 0.26 X_2X_3 - 15.97\,X_1^2 - 23.89\,X_2^2 - 12.94\,X_3^2 \quad (4)$$

The R^2, R^2 (adjusted) and R^2 (predicted) were 0.9613, 0.9265 and 0.9479, respectively. In experimental design, R^2 is an estimate of amount of variation around the mean described by the model. By adding factors to the model, R^2 always increases whether the added factor is significant or not (Myers Raymond and Montgomery, 2002). And, R^2 indicated that 96.13% of the variability in the data was attributed to the model. The coefficient of determination R^2 adj for the above predicting Eq.(4) was 0.9265. Therefore, this quadratic equation can be used for predicting response at any combination of three variables in the experimental range.

Fig. 3 exhibits the 3D response surface plot of the effects of temperature (°C), urea (g l^{-1}), and peptone (g l^{-1}) on the urea degradation efficiency. The urea degradation efficiency showed a parabolic trend with the increases of temperature, urea, and peptone. In other words, the urea

degradation efficiency was firstly increased to a maximum and then decreased with the further increases of three variables. Accordingly, and an optimal ranges of three variables can be accordingly predicated to optimize urea degrading performance. From the response surface, it was concluded that the optimal ranges of the process parameters for maximum urea degradation efficiency were temperature = 28-31 °C, urea = 4.8-5.6 g l^{-1}, peptone = 6.2-8.1 g l^{-1}.

3.4 Calcite precipitates

During the growth of the mutant LHUM107 with urea as the sole nitrogen source, Ca^{2+} could be removed by precipitation if existed. According to previous researches, biological and chemical processes were both involved. Firstly, urea is degraded mediated by the urease expression in the strain. The ending products include NH_3 and CO_2, in which NH_3 dissolves in water to produce NH_4^+ and OH^- and CO_2 dissolves in water to produce CO_3^{2-}. Under basic conditions, CO_3^{2-} and Ca^{2+} would react to form $CaCO_3$ precipitates, removing Ca^{2+} from the solution (Kayastha and Das, 1999). In the assays, Ca^{2+} was added at a theoretical dosage. After 48 h of cultivation, a certain amount of precipitates tightly adhered to the surface of mutant cells. Lochhead *et al.* (1997) investigated the interaction of organic-inorganic interface and noted that a single membrane with negative charges would favor the crystal nucleation and growth. In general, cell surface is negatively charged, which tends to attract positively-charged Ca^{2+} moving close. And the precipitation is likely to occur on the bacterial surface or nearby. Bacteria probably provide nucleation sites for $CaCO_3$, leading to the co-precipitation with $CaCO_3$. In this study, the EDS and XRD results both confirmed that $CaCO_3$ was only form of these precipitates, exactly approving above supposition.

During the precipitation of $CaCO_3$, many environmental conditions would directly influence

the crystal morphology of the resulted precipitates (Hu and Deng, 2003; Kitamura *et al.*, 2002). For example, as imaging by SEM, the presence of cells would cause an uninformed shape of the crystals. The previous experiments had demonstrated that the mutant LHUM107 was capable of excreting extracellular urease for the degradation of urea (data was not shown). Therefore, extracellular urease of the strain LHUM107 was extracted to induce the precipitation of $CaCO_3$. The EDS and XRD results illustrated the precipitates formed with the extracted extracellular urease, which were similar to the crystals that Bang and Ramakrishnan (2001) obtained via *Bacillus pasteurii* induced $CaCO_3$ precipitation during the microbiologically-enhanced crack remediation (MECR). Based on Tong *et al.* (2004), the precipitates were typical calcite crystal in the form of multi-layered $CaCO_3$. The results of EDS and XRD documented the mineral phase of $CaCO_3$.

In the assay, precipitation of $CaCO_3$ was achieved by the extraction of extracellular components. This indicates that the urease produced by the mutant LHUM107 was an extracellular enzyme. The urease generated by many genus microbes is located on the cell membrane or interlayer space, with some exceptions (*Helicobacter pylori*) that excrete urease to extracellular space based on their special selective mechanisms (Vanet and Labigne, 1998). The decomposition of urea to NH_3 and CO_2 by LHUM107 was a reaction occurring out of the cell, which enabled the precipitation of $CaCO_3$ using the extracted urea to avoid the interface of bacterium cells. As illustrated in Fig. 4, the concentration of Ca^{2+} in the solution decreased from 11100.00 mg l^{-1} to 947.17 mg l^{-1} in 6 h with the aid of extracellular urease, corresponding to a removal efficiency of 91.5%. Comparing with the precipitation with cell suspension (Stocks-Fischer *et al.*, 1999), this technology made a faster $CaCO_3$ precipitation, which is very

beneficial for the real application of the extracellular extract from the urease-producing strain.

Conclusions

This study isolates another *Baccillus* strain with urease expression capacity, that was used as starting strain for the investigation of calcite precipitation. The ultraviolet mutagenesis was induced to advance urease expression in terms of urea-degrading capability, and a mutant LHUM107 with promising genome stability was consequently obtained. Adapting to the optimal conditions from RSM, the extracellular urease showed more promising calcite precipitation performances than bacterial suspension of mutant LHUM107, and $CaCO_3$ was identified as only form in these precipitates.

Acknowledgements

This work was financially supported by the National Natural Science Foundation of China (No. 30970152).

Appendix A. Supplementary data

Supplementary data associated with this article can be found in the online version.

References

1. Bang, S.S., Ramakrishnan, V., 2001. Microbiologically enhanced crack remediation (MECR). Proceedings of the international symposium on industrial application of microbial genomes. Daegu, Korea. 3-13.

2. Baskar, S., Baskar, R., Mauclaire, L., McKenzie, J., 2006. Microbially induced calcite precipitation in culture experiments: Possible origin for stalactites in Sahastradhara caves, Dehradun, India. Current science, 90, 58-64.

3. Cheng, L., Cord-Ruwisch, R., 2012. In situ soil cementation with ureolytic bacteria by surface

percolation. Ecol. Eng. 42, 64-72.

4. De Beer, D., Larkum, A., 2001. Photosynthesis and calcification in the calcifying algae *Halimeda discoidea* studied with microsensors. Plant, Cell & Environ. 24, 1209-1217.

5. DeJong, J.T., Fritzges, M.B., Nüsslein, K., 2006. Microbially induced cementation to control sand response to undrained shear. J. Geotech. Geoenviron. 132, 1381-1392.

6. Ferris, F., Phoenix, V., Fujita, Y., Smith, R., 2004. Kinetics of calcite precipitation induced by ureolytic bacteria at 10 to 20 °C in artificial groundwater. Geochim. Cosmochim. Ac. 68, 1701-1710.

7. Hu, Z., Deng, Y., 2003. Supersaturation control in aragonite synthesis using sparingly soluble calcium sulfate as reactants. J. Colloid Interf. Sci. 266, 359-365.

8. Jaliliannosrati, H., Amin, N.A.S., Talebian-Kiakalaieh, A., Noshadi, I., 2013. Microwave assisted biodiesel production from *Jatropha Curcas* L. seed by two-step in-situ process: Optimization using response surface methodology. Bioresour. Technol. 136, 565-573.

9. Jiménez-López, C., Rodriguez-Navarro, C., Piñar, G., Carrillo-Rosúa, F., Rodriguez-Gallego, M., Gonzalez-Muñoz, M., 2007. Consolidation of degraded ornamental porous limestone stone by calcium carbonate precipitation induced by the microbiota inhabiting the stone. Chemosphere. 68, 1929-1936.

10. Kayastha, A.M., Das, N., 1999. A simple laboratory experiment for teaching enzyme immobilization with urease and its application in blood urea estimation. Biochem. Educ. 27, 114-117.

11. Kim, H., Park, S., Han, J., Lee, H., 2013. Microbially mediated calcium carbonate precipitation on normal and lightweight concrete. Constr. Build. Mater. 38, 1073-1082.

12. Kitamura, M., Konno, H., Yasui, A., Masuoka, H., 2002. Controlling factors and mechanism of reactive crystallization of calcium carbonate polymorphs from calcium hydroxide suspensions. J. Cryst. Growth. 236, 323-332.

13. Lochhead, M.J., Letellier, S.R., Vogel, V., 1997. Assessing the role of interfacial electrostatics in oriented mineral nucleation at charged organic monolayers. J. Phys. Chem. B. 101, 10821-10827.

14. Mobley, H., Hausinger, R., 1989. Microbial ureases: significance, regulation, and molecular characterization. Microbiol. Rev. 53, 85-108.

15. Myers Raymond, H., Montgomery, D.C., 2002. Response surface methodology: process and product optimization using designed experiment. A Wiley-Interscience Publication.

16. Nakano, H., Takenishi, S., Watamabe, Y., 1984. Purification and properties of urease from *Brevibacterium ammoniagenes*. Agric. Biol. Chem. 48, 1495-1502.

17. Rahman, M.A., Oomori, T., Uehara, T., 2008. Carbonic anhydrase in calcified endoskeleton: novel activity in biocalcification in alcyonarian. Mar. Biotechnol. 10, 31-38.

18. Riding, R., 2000. Microbial carbonates: the geological record of calcified bacterial-algal mats and biofilms. Sedimentology. 47, 179-214.

19. Rivadeneyra, M.a.A., Delgado, G., Soriano, M., Ramos-Cormenzana, A., Delgado, R., 2000. Precipitation of carbonates by *Nesterenkonia halobia* in liquid media. Chemosphere. 41, 617-624.

20. Rodriguez-Navarro, C., Jimenez-Lopez, C., Rodriguez-Navarro, A., Gonzalez-Muñoz, M.T., Rodriguez-Gallego, M., 2007. Bacterially mediated mineralization of vaterite. Geochim. Cosmochim. Ac. 71, 1197-1213.

21. Rokita, E., Makristathis, A., Hirschl, A.M., Rotter, M.L., 2000. Purification of surface-associated urease from *Helicobacter pylori*. J. Chromatogr. B: Biomed. Sci. Appl. 737, 203-212.

22. Soon, N.W., Lee, L.M., Khun, T.C., Ling, H.S., 2013. Improvements in engineering properties of soils through microbial-induced calcite precipitation. KSCE J. Civ. Eng. 17, 718-728.

23. Stocks-Fischer, S., Galinat, J.K., Bang, S.S., 1999. Microbiological precipitation of $CaCO_3$. Soil Biol. Biochem. 31, 1563-1571.

24. Thomas, L., Chamberlin, G., 1974. Colorimetric chemical analysis methods. Tintometer Ltd., Salisbury, England.

25. Thornley, J.H., France, J., 2005. An open-ended logistic-based growth function. Ecol. Model. 184, 257-261.

26. Tong, H., Ma, W., Wang, L., Wan, P., Hu, J., Cao, L., 2004. Control over the crystal phase, shape, size and aggregation of calcium carbonate via a L-aspartic acid inducing process. Biomaterials. 25, 3923-3929.

27. Vanet, A., Labigne, A., 1998. Evidence for specific secretion rather than autolysis in the release of some *Helicobacter pylori* proteins. Infect. Immun. 66, 1023-1027.

28. Verhulst, P. F., 1838. Notice sur la loi que la population suit dans son accroissement. Correspondance Mathématique et Physique Publiée par A. Quetelet, 10, 113-121.

29. Wan, C., Yang, X., Lee, D.-J., Du, M., Wan, F., Chen, C., 2011. Aerobic denitrification by novel isolated strain using as nitrogen source. Bioresour. Technol. 102, 7244-7248.

30. Witkin, E.M., 1976. Ultraviolet mutagenesis and inducible DNA repair in *Escherichia coli*. Bacteriol. Rev. 40, 869-907.

31. Wu, C. Y., Peng, Y. Z., Wang, S. Y., Ma, Y., 2010. Enhanced biological phosphorus removal by granular sludge: From macro-to micro-scale. Water Res. 44, 807-814.

32. Zhou, X., Xin, Z. J., Lu, X. H., Yang, X. P., Zhao, M. R., Wang, L., Liang, J. P., 2013. High efficiency degradation crude oil by a novel mutant irradiated from *Dietzia* strain by 12C6+ heavy ion using response surface methodology. Bioresour. Technol. 137, 386-393.

Figure Captions

Figure 1 Phylogenetic tree for starting strain LH1.

Figure 2 Cell growth and urea degradation (A) and genome stability of mutant LHUM107 (B).

Figure 3 Response surfaces of urea degradation efficiency as a function of temperature, urea, peptone: (A) temperature and urea; (B) temperature and peptone; (C) urea and peptone.

Figure 4 Changes of calcium concentration by extracellular urease.

Table 1 Actual values and levels values of the variables employed in RSM.

Variables	Range and level		
	-1	0	+1
X_1/Temperature (°C)	20	30	40
X_2/Urea (g l^{-1})	1	5.5	10
X_3/Peptone (g l^{-1})	0.5	5.25	10

Table 2 ANOVA for response surface reduced quadratic model.

Source	Sum of squares	df	Mean square	F-vaue	p-Value Prob>F	
Model	19553.63	9	2172.63	5.12	0.0088	Significant
X_1-temperature	981.33	1	981.33	2.31	0.1592	
X_2-urea	3736.13	1	3736.13	8.81	0.0141	
X_3-peptone	93.16	1	93.16	0.22	0.6493	
$X_1 X_2$	167.72	1	167.72	0.40	0.5435	
$X_1 X_3$	0.53	1	0.53	1.247E-003	0.9725	
$X_2 X_3$	173.00	1	173.00	0.41	0.5374	
X_1^2	5034.92	1	5034.92	11.87	0.0063	
X_2^2	8949.24	1	8949.24	21.10	0.0010	
X_3^2	3013.80	1	3013.80	7.11	0.0237	
Residual	4240.61	10	424.06			
Lack of Fit	4213.17	5	842.63	153.54	<0.0001	Significant
Pure Error	27.44	5	5.49			
Cor Total	23794.24	19				
R^2=0.9613		R^2(adjusted)=0.9265			R^2(predicted)=0.9479	

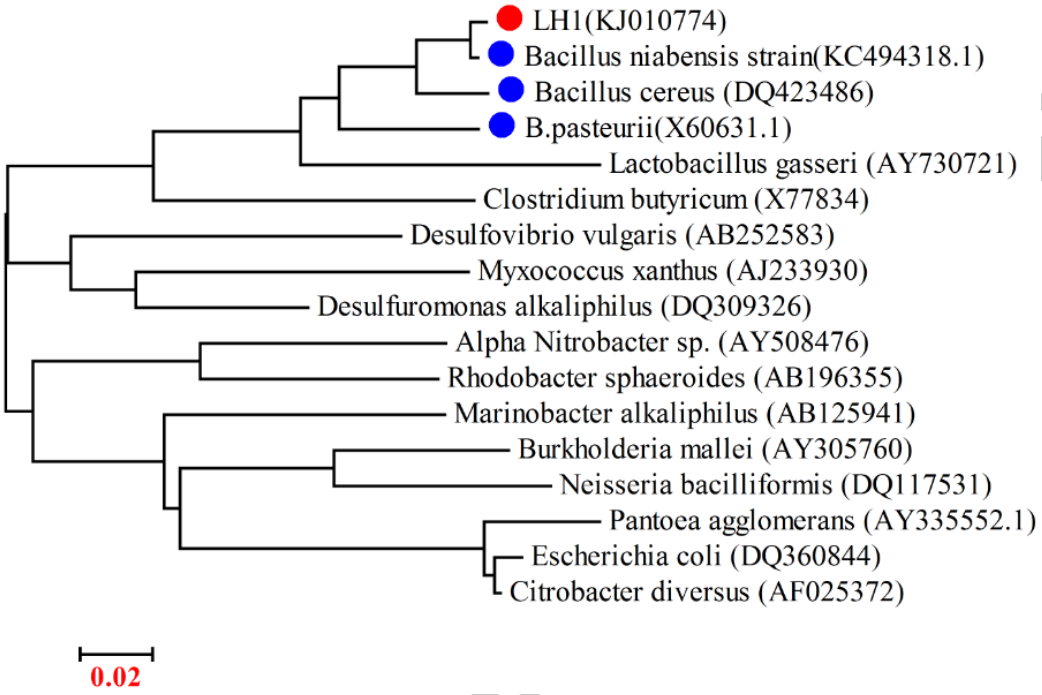

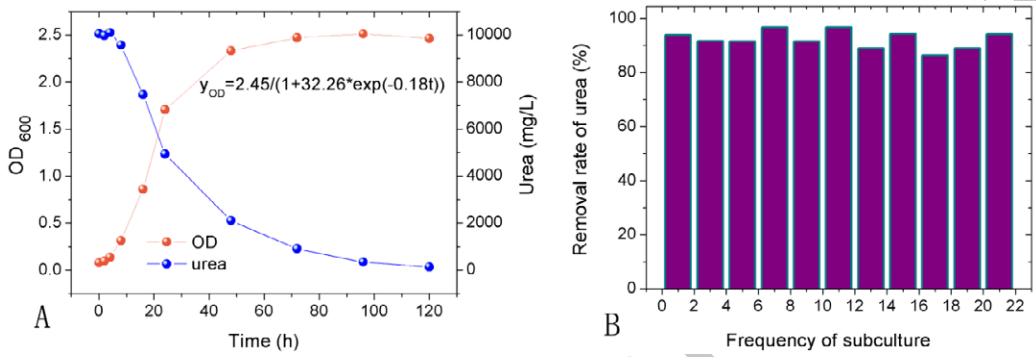

(A)

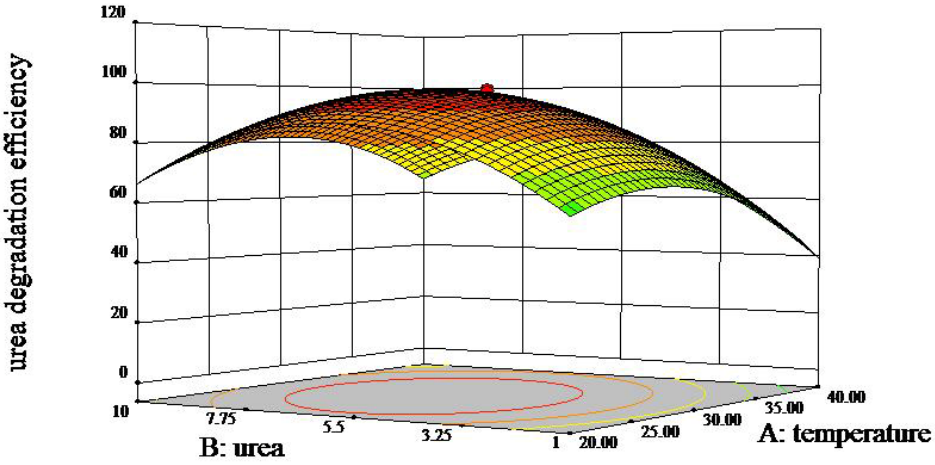

(B)

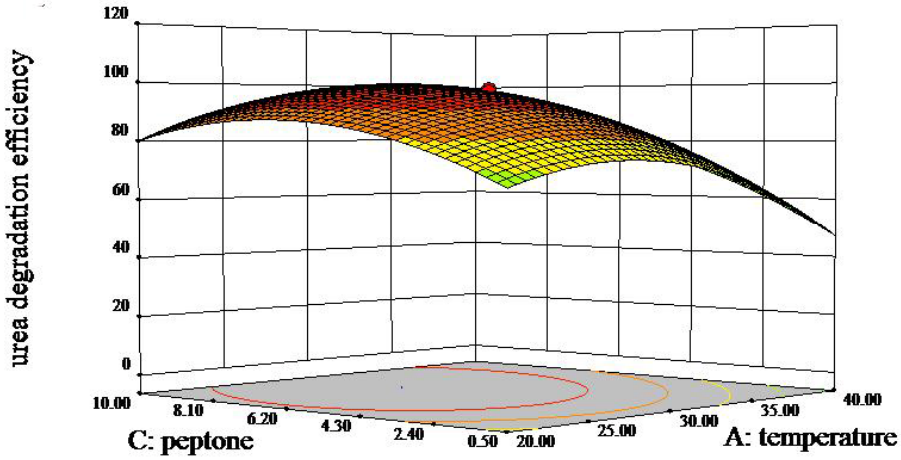

(C)

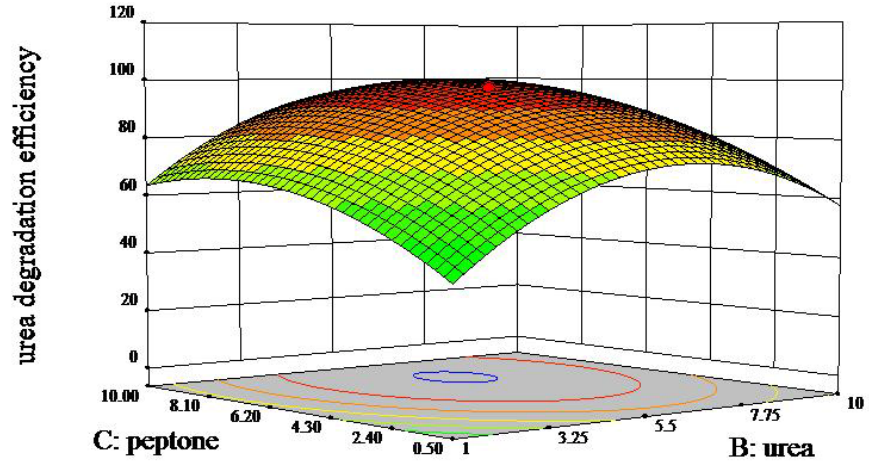

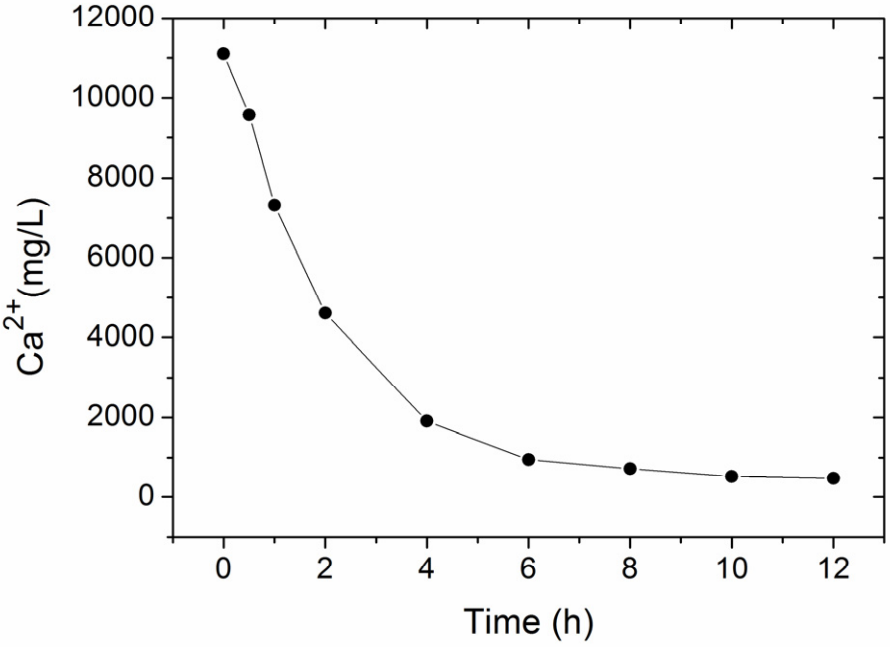

Graphical Abstract

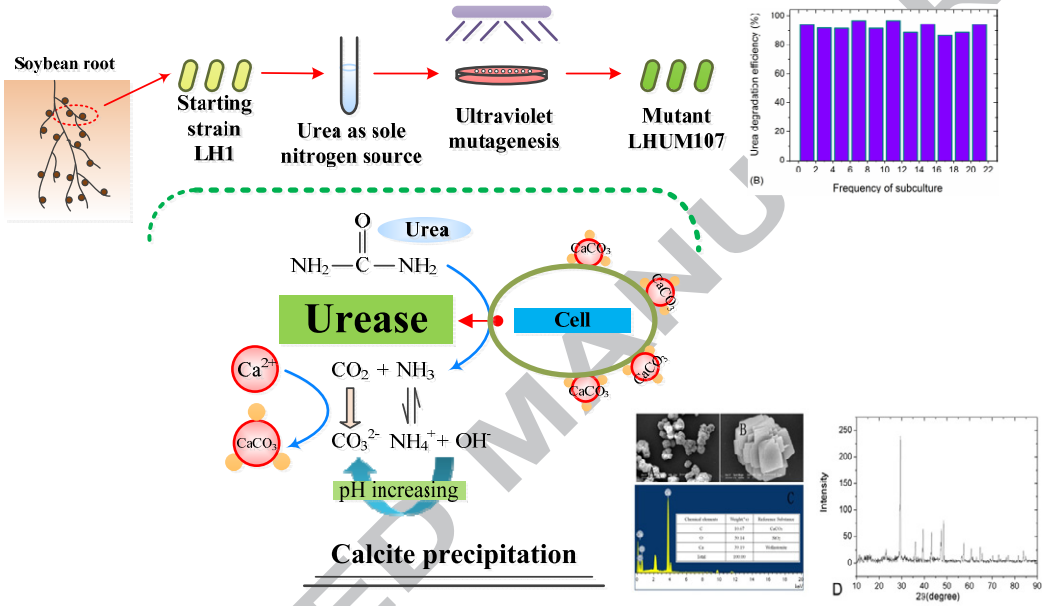

Highlights

- An effective urea-degrading strain LH1 was isolated from soil on soybean root.
- The mutant LHUM 107 exhibited outstanding calcite precipitation ability.
- Response surface methodology brought forward the optimal conditions.
- Extracellular urease was more effective targeted for $CaCO_3$ precipitation.